Article:
Li, C, Holden, J and Grayson, R (2019) Sediment and fluvial particulate carbon flux from an eroding peatland catchment. Earth Surface Processes and Landforms, 44 (11). pp. 2186-2201. ISSN: 0197-9337

https://doi.org/10.1002/esp.4643

Sediment and fluvial particulate carbon flux from an eroding peatland catchment

Changjia Li*, Joseph Holden and Richard Grayson

water@leeds, School of Geography, University of Leeds, Leeds, LS2 9JT, UK.

*Correspondence to: Changjia Li, School of Geography, University of Leeds, Leeds, LS2 9JT, UK. E-mail: changjia.li@hotmail.com; gycl@leeds.ac.uk

Abstract

Erosion and the associated loss of carbon is a major environmental concern in many peatlands and remains difficult to accurately quantify beyond the plot scale. Erosion was measured in an upland blanket peatland catchment (0.017 km^2) in northern England using Structure-from-Motion (SfM) photogrammetry, sediment traps and stream sediment sampling at different spatial scales. A net median topographic change of –27 mm yr^{-1} was recorded by SfM over the 12-month monitoring period for the entire surveyed area (598 m^2). Within the entire surveyed area there were six nested catchments where both SfM and sediment traps were used to measure erosion. Substantial amounts of peat were captured in sediment traps during summer storm events after two months of dry weather where desiccation of the peat surface occurred. The magnitude of topographic change for the six nested catchments determined by SfM (mean value: 5.3 mm, standard deviation: 5.2 mm) was very different to the areal average derived from sediment traps (mean value: –0.3 mm, standard deviation: 0.1 mm). Thus direct interpolation of peat erosion from local net topographic change into sediment yield at the catchment outlet appears problematic. Peat loss measured at the hillslope scale was not representative of that at the catchment scale. Stream sediment sampling at the outlet of the research catchment (0.017 km^2) suggested that the yields of suspended sediment and particulate organic carbon were 926.3 t km^{-2} yr^{-1} and 340.9 t km^{-2} yr^{-1} respectively, with highest losses occurring during the autumn. Both freeze–thaw during winter and desiccation during long periods of dry weather in spring and summer were identified as important peat weathering processes during the study. Such weathering was a key enabler of subsequent fluvial peat loss from the catchment.

KEYWORDS: erosion; Structure-from-Motion; topographic change; desiccation; wetland

Introduction

Peatlands cover approximately 4.23 million km^2 (2.84%) of the world's land area (Xu et al., 2018b). They store an equivalent of around two thirds of carbon stored in the atmosphere (Yu et al., 2010). Peatlands in the UK are highly valued because they provide a wide range of ecosystem services such as water supply (Xu et al., 2018a), biodiversity and recreation (Holden et al., 2007, Bonn et al., 2009) and the largest terrestrial carbon pool (Cannell et al., 1993, Milne and Brown, 1997). Though peatlands form an important carbon reserve, they can be degraded under a wide range of internal and external pressures (Parry et al., 2014). Numerous studies have suggested that peatlands can be both sinks and sources of carbon to the environment (Clay et al., 2012, Holden et al., 2007). Land management practices and pollution have led to disturbance of peat surfaces, resulting in large areas being extensively eroded (Li et al., 2016b, Li et al., 2018a) or under increasing erosion risk (Li et al., 2016a, Li et al., 2017) in many peatlands of the UK. The physical disturbance of peat by weathering processes (e.g., freeze–thaw and desiccation) and erosive forces (e.g., water and wind) has the potential to considerably affect the ability of peat to sequester carbon (Evans and Warburton, 2007).

Fluvial organic carbon fluxes in both particulate and dissolved forms are important links between terrestrial peatland carbon stores and the ocean carbon sink (Hope et al., 1997, Goulsbra et al., 2016, Stimson, 2016). Fluvial carbon is also subject to oxidation representing an important link between terrestrial and atmospheric carbon pools (Pawson et al., 2012, Shuttleworth et al., 2015). While dissolved organic carbon (DOC) fluxes have been well studied (e.g., Worrall et al. (2003), Worrall et al. (2009), Evans et al. (2006)), particulate organic carbon (POC) losses from peatlands has been

much less studied (Pawson et al., 2012, Billett et al., 2010). In less severely eroded or intact peatland systems, POC is usually 5–50% of the total organic carbon load (Hope et al., 1997, Dawson et al., 2002). However, for eroding headwater catchments the POC flux represents an even larger proportion of fluvial organic carbon export (Pawson et al., 2008, Evans and Warburton, 2005). For example, Pawson et al. (2008) reported that POC flux from an eroding site in the English Peak District represented over 80% of the total organic carbon fluxes (107 g C m^{-2} yr^{-1}) from the system. A similar magnitude of POC flux has been historically reported from other eroding peat systems in northern England (Crisp, 1966, Evans and Warburton, 2005). In headwater systems, active erosion forms such as gullies typically export large amounts of POC to peatland streams (Evans et al., 2006, Evans and Warburton, 2007, Evans and Lindsay, 2010). Assessing the temporal patterns of POC from eroding peatlands has the potential to provide insight into the controls on fluvial carbon flux from these systems (Pawson et al., 2012, Shuttleworth et al., 2015). It can also provide important baseline data to assess effects of restoration projects on carbon fluxes in the fluvial system.

Weathering processes such as frost action and desiccation play an important role in supplying erodible peat particles for fluvial transport (Shuttleworth et al., 2017, Li et al., 2018a). Frost weathering - resulting from the freezing and thawing of water between peat particles - is common in cool, high latitude or high altitude climates which support many peatlands. This frost action plays a vital role in breaking up the peat surface during winter months (Francis, 1990, Labadz et al., 1991, Li et al., 2018b). A major form of frost weathering on peat is needle-ice which is important in producing eroding peat faces (Tallis, 1973, Luoto and Seppälä, 2000, Grab and Deschamps, 2004) with ice crystal growth gradually weakening and finally breaking peat soil

92 aggregates and the subsequent warming and thawing weakening or loosening the
93 fractured peat. The growth of needle ice can lead to a 'fluffy' peat surface that is loose
94 and granular and vulnerable to being flushed off by overland flow events (Li et al.,
95 2018b, Evans and Warburton, 2007). Surface desiccation during extended periods of
96 dry weather is another important weathering process for producing erodible peat (Burt
97 and Gardiner, 1984, Evans et al., 1999, Francis, 1990, Holden and Burt, 2002).
98 Francis (1990) monitored erosion in a mid-Wales blanket peat catchment (Plynlimon)
99 during two drought years (1983–1984) and found that frost action appeared to be of
100 relatively little importance; and instead summer desiccation was far more significant.
101 Li et al. (2016a) modelled the effect of future climate change on UK peatlands and
102 found that peat desiccation is likely to become more important in blanket peatlands as
103 a result of warmer summers. However, additional field monitoring data is required to
104 parameterize models of the temporal dynamics of peat erosion and their responses to
105 climate change (Li et al., 2017).
106 Different peat erosion processes are active at different spatial scales (Li et al.,
107 2018a). For example, rainsplash, interrill and rill erosion are the dominant erosion
108 processes studied at fine scales (erosion plots) (Holden et al., 2008, Li et al., 2018c,
109 Li et al., 2018b, Holden and Burt, 2002, Grayson et al., 2012). For larger hillslopes and
110 small and medium-size catchment scales (1000 m^2 – 1 ha), gully erosion and mass
111 movements become more important, yielding large quantities of sediment (Evans and
112 Warburton, 2007, Evans et al., 2006, Evans and Warburton, 2005). At the large basin
113 scale (> 1 ha) long-term (> 1 year) erosion and sediment deposition processes are
114 potentially more important due to large sediment sinks (footslopes and floodplains)
115 (De Vente and Poesen, 2005). Further research is needed on the role of streams as
116 sediment sources and (temporal) sinks. Multi-scale studies to facilitate spatial

upscaling of erosion rates and provide data on the spatial connections between different units at each scale are necessary.

This paper addresses the key knowledge gaps by assessing the hydrosedimentary dynamics of a peat-dominated catchment over the course of a year. The specific objectives are to: (i) measure fluvial suspended sediment and POC fluxes from an eroding headwater peatland system; (ii) describe the dynamics of suspended sediment transport at different temporal scales (seasonal and monthly); and (iii) compare peat erosion rates measured by different techniques (sediment traps, SfM photogrammetry, sediment sampling) at different scales (plot, mini-catchment and catchment).

Materials and methods

Study area

Extensive peat erosion in the UK occurs across many upland systems but particularly in the Pennine region of England (Bower, 1960b, Bower, 1961, Evans and Warburton, 2007). Fleet Moss (54°14´55´´N, 2°12´53´´W) is an area of approximately 1.0 km^2 with blanket peat deposits of up to 2m depth, at an altitude of 550–580 m in the Yorkshire Dales National Park in North Yorkshire, England (Figure 1). The vegetation is dominated primarily by *Eriophorum vaginatum*, *Calluna vulgaris* and *Empetrum nigrum*. The research catchment (0.017 km^2) within Fleet Moss (Figure 2) has a large area of exposed bare peat covering 60% of the catchment, as estimated from aerial images. There are a range of erosion forms (interrill and rill erosion and gullying). There are well developed and connected Type 1 and Type 2 gully systems as classified by Bower (1960a). On the flatter interfluve areas (slopes less than 5°), Type 1 dissection usually occurs with gullies branching and intersecting in an intricate

142 dendritic network. On steeper slopes (exceeding 5°), Type 2 dissection dominates with
143 a system of sparsely branched drainage gullies incised through the peat and aligned
144 nearly parallel to each other.

145 < Figure 1 is here >

146

147 Data acquisition: monitoring and sampling

148 Data on climate parameters, discharge, sediment, POC and topographic changes
149 were collected between October 2016 and November 2017. Discharge, sediment and
150 POC were measured at the outlet of the research catchment (1.7 ha). For a 990 m^2
151 area within the 1.7 ha catchment, sediment was collected by traps and SfM surveys
152 were conducted.

153

154 Climate data

155 Rainfall was logged every 15 minutes with a tipping bucket raingauge during the
156 course of the study. Temperature for the air and soil was measured using Tinytag Plus
157 2 loggers (resolution 0.01 ºC) at 10-minute intervals from 26/10/2016 to 20/07/2017
158 after which a logger failure meant data collection ceased. The air temperature sensor
159 was housed in a radiation shield approximately 1.5 m above the ground surface. The
160 soil temperatures sensors were located at surface, 5 cm and 10 cm depths.

161

162 Topographic change measured by SfM photogrammetry

163 SfM photogrammetry is a technique that is low cost and quick to use in terms of data
164 acquisition and post-processing and thus was used to measure topographic change.
165 Over the study period (26/10/2016–02/11/2017), a mini-catchment (990 m^2) was
166 surveyed six times (Table 1). Since weather conditions during field campaigns

167 significantly influence data quality (Snapir et al., 2014, Stöcker et al., 2015), image
168 acquisition was arranged under conditions with no rain, no snow cover or no sunny
169 weather to avoid producing strong shadows on images. Areas near the catchment
170 boundary were subject to poorer quality SfM data (point clouds were sparse with large
171 empty areas or vegetated points). Therefore, the SfM data analysis focused on a 598
172 m^2 central part of the catchment (yellow boundary shown in Figure 2).

173 < Figure 2 is here >

174 < Table 1 is here >

175 Abundant high-quality images were taken at positions and angles that have
176 sufficient coverage of the peat erosion features of interest. In specific erosion features
177 (i.e. gully heads, peat hagg), the density of images from additional perspectives was
178 increased for further detailed reconstruction. The camera used was a Sony ILCE-6000
179 24 mega pixel digital camera with a 16 mm focal length. Camera settings varied based
180 on light conditions, with exposure between 160 and 320 ISO, F-stop between f/4 and
181 f/4.5 and exposure time between 1/160 and 1/80 second. Fourteen permanent Ground
182 Control Points (GCPs) made of rebar (0.5–1.0 m in length) with a painted white top
183 (high contrast with the dark peat surface) were placed around and within the feature
184 of interest. The rebar was hammered deep into the substrate below the peat. A
185 geodimeter was used and full surveys of the relative coordinates of all the GCPs were
186 carried out at the start of the monitoring period.

187 Images acquired were processed using the commercial software Agisoft PhotoScan,
188 to produce a dense point cloud based on the workflows described in Li et al. (2019).
189 Poorly located GCPs were excluded; however, a minimum of six GCPs that were well
190 distributed over each site remained (Fonstad et al., 2013, Smith et al., 2014). Point-
191 cloud quality was evaluated by summarizing residual errors using root mean squared

error (*RMSE*) (Smith et al., 2014), and mean georeferencing uncertainty was 40.5 mm (Table 1). The derived dense point clouds contained both bare peat surface and vegetation points. Vegetation was filtered through selecting vegetation points based on RGB values embedded in the point cloud and the filtering was conducted in the open source CloudCompare software. Cloud-to-cloud differencing was computed using the Multiscale Model to Model Cloud Comparison (M3C2) algorithm that quantifies 3-D distance between two point clouds along the normal surface direction and provide a 95% confidence interval based on the point cloud roughness and co-registration uncertainty (Lague et al., 2013). M3C2 requires two main user-defined parameters: i) the normal scale *D*, which is used to calculate a surface normal for each point and is dependent upon surface roughness and registration error; ii) the projection scale *d* within which the average surface elevation of each cloud is calculated. In this study, the normal scale *D* for each point cloud was estimated based on a trial-and-error approach similar to that of Westoby et al. (2016) and was fixed at 0.5 m. The projection scale *d* was specified as 0.1 m and this scaling was enough to average a minimum of 30 points sampled in each cloud (Lague et al., 2013). M3C2 output was subsequently masked to exclude points where change is lower than level of Level of Detection (LoD) threshold for a 95% confidence level ($LoD_{95\%}$), which is defined as:

$$LOD_{95\%}(d) = \pm 1.96\left(\sqrt{\frac{\sigma_1(d)^2}{n_1} + \frac{\sigma_2(d)^2}{n_2}} + reg\right) \quad (1)$$

where σ_1 and σ_2 represent the roughness of each point in sub-clouds of diameter *d* and size n_1 and n_2, and *reg* is the user-specified registration error which is assumed to be isotropic and spatially uniform across the dataset (Lague et al., 2013). The surface-to-surface Interactive Closest Point algorithm implemented in CloudCompare was used to align a patch of two inactive point clouds. The registration error was

estimated by a series of tests and it ranged from 7.0 to 8.0 mm for the field models. Data analyses were conducted between individual survey dates with dates and intervals presented in Table 1. Between 26/10/2016 and 02/11/2017 the 6 repeat topographic surveys yielded 5 survey intervals (e.g., 2–1; 3–2), and a long-term survey interval (6–1) which was selected to represent potential large topographic changes.

DEMs were derived from the dense point clouds gridded at 0.01 m. The DEM data used a relative coordinate system, with the point clouds georeferenced using local GCPs. Two transect profiles (Figure 2) were selected to extract data from the DEMs to reveal the changes in relative coordinates.

Peat eroded through fluvial processes

A series of sediment traps (Baynes, 2012, Fewings, 2014) were used to measure the quantity of peat eroded by fluvial processes from different parts of the catchment from 04/11/2016 to 21/08/2017 (Figure 2). The traps were made of weaved polypropylene bags which allow water to drain through the sack, but ensure any peat transported in suspension is trapped. The trapping efficiency was assessed in the laboratory by pouring 1 L peat solution (100 g L^{-1}) into a polypropylene bag over a plastic box and allowing water to seep for 24 hours. The collected solution was poured into weighed beakers, oven-dried, and weighed. The trapping efficiency of the sacks determined by this experiment was 91.7 ± 0.5 %. In the field the trapped peat materials were weighed as field moisture weight. Five subsamples were collected and sealed in plastic bags, returned to the laboratory, oven-dried, and weighed. The moisture contents of the subsamples were calculated, then averaged and multiplied by the field moisture peat

240 weight, allowing the estimation of field dried peat weight. The traps installed in the field
241 were renewed periodically.
242
243 Stream discharge and catchment sediment yield
244 Steam discharge (Q) was monitored at a cross-section with a 'U' shape at the outlet
245 of the research catchment (1.7 ha) using automatic pressure sensors. Unfortunately
246 the water level data collected by the logger could not be used as the shallow nature of
247 the channels resulted in poor quality data due to issues with temperature
248 compensation. Therefore daily discharge data were interpolated from the rainfall-
249 runoff relationship (rainfall x study area). Previous studies in UK headwater blanket
250 peatlands have shown the runoff coefficient to be > 80% (Evans et al., 1999, Holden
251 et al., 2012, Marc and Robinson, 2007, Holden et al., 2017). Evapotranspiration is
252 expected to be low over the research catchment used in this study due to large areas
253 of bare peat. The runoff coefficient was therefore assumed to be 0.9 in this small
254 headwater peatland catchment.
255 An automatic pump sampler (ISCO 6712C) was used to take samples once per day
256 at 13:00 (UTC +2) from 26 October 2016 to 01 November 2017. Samples were filtered
257 through Whatman GF/F 47 mm (0.7 µm) circle filter papers in the laboratory. Total
258 suspended sediment concentrations (SSCs) were measured by oven-drying at 105 °C
259 to constant weight. All water samples contained both inorganic and organic fractions.
260 POC was determined by first conducting loss-on-ignition tests in a muffle furnace at
261 375 °C for 16 hours to give organic matter content that was then converted to POC
262 using the method of Ball (1964).
263 The suspended sediment yield (Q_s: kg d^{-1}) was calculated by $Q_s = SSC \times Q$, where
264 SSC (kg m^{-3}) and Q (m^3 d^{-1}) are suspended sediment concentration and discharge,

respectively. The values of suspended sediment yield Q_s were regressed against discharge Q using measured daily data for different months and the total study period. A power function, $Q_s = aQ^b$, widely used to estimate transport, where a and b are empirical constants, was applied to form a Q_s fit for different events and months. The POC yield (Q_{POC}: kg d^{-1}) and the rating curve for Q_{POC} were calculated in the same way with Q_s.

Data analysis

Peat loss obtained from SfM was converted to an estimate of weight loss using peat bulk density values from the study site. Regression analysis was used to identify the relationship between SS or POC loads and daily discharge. Test results were considered significant at $p < 0.05$. The area-specific sediment yields measured from plots, a series of nested mini-catchments, and stream sampling measurements for the whole study area were compared.

Results

Peat surface topographic change measured by SfM

M3C2 differences above Level of Detection threshold at 95% confidence level ($LoD_{95\%}$) over different survey intervals are given in Table 2. The spatial distribution and histogram of M3C2 differences for different comparisons are shown in Figure 3. M3C2 distances ranged from negative values marked with red colour to positive values marked with blue colour. In this study the 'positive M3C2 distance' more accurately reflects topographic change that could be caused by both deposition and swelling processes; while 'negative M3C2 distance' could also be attributed to both erosion

289 and shrink processes (Grayson et al., 2012, Evans and Warburton, 2007, Glendell et
290 al., 2017).

291 < Table 2 is here >

292 From 04/11/2016 to 02/05/2017, there were large areas of the peat surface (69%)
293 showing significant change (i.e. M3C2 distance > $LoD_{95\%}$). Net topographic change
294 was –18 mm, with a high variability as shown in the large root mean square (RMS) of
295 the M3C2 distance which was 85 mm (Table 2). The magnitude of the negative
296 topographic change yielded a median change of 65 mm, which was much greater than
297 the median positive topographic change (50 mm) (Table 2). This period had the
298 greatest total rainfall but low rainfall intensity and 57 days of temperatures below 0 ºC.
299 These conditions may cause surface expansion due to freezing. The spatial variability
300 of the changes showed that negative topographic change mainly occurred on
301 hillslopes along the main stream networks (Figure 3 (a)), with 52% of the total area
302 that is above the $LoD_{95\%}$ (Table 2). In contrast, positive topographic change was found
303 predominantly on the north-east, north-west and southern edge areas of the
304 catchment (Figure 3 (a)) where overland flow paths were not connected and bare peat
305 areas are surrounded by dense vegetation cover (Figure 2).

306 The next survey interval (Model 3–2: 02/05/2017–13/06/2017) experienced greater
307 topographic changes in both magnitude (median = –29 mm) and extent (77% of the
308 total area = 461.8 m^2) (Table 2) than the first survey interval (Model 2–1). The positive
309 topographic change was observed in the upper stream areas, i.e. north-east and south
310 parts of the catchment (Figure 3 (b)). Model 4–3 (from 13/06/2017 to 21/08/2017) had
311 a longer time interval (70 days) than the previous interval (Model 3–2, 43 days), but
312 displayed smaller areas with significant topographic changes (72%) within the
313 catchment (Table 2). Positive topographic change was more extensive (60% of the

area), leading to a net positive topographic change (Table 2 and Figure 3 (c)). A small zone of negative change was evident in the central-south part of the study area (Figure 3 (c)). For Model 5–4 (21/08/2017–27/09/2017), 73% of the area is above the $LoD_{95\%}$, among which 60% of the area is dominated by negative topographic change. Finally, the survey interval from 27/09/2017 to 02/11/2017 (Model 6–5) demonstrated 73% of the catchment area had significant change.

< Figure 3 is here >

The topographic change between the first survey (04/11/2016) and last survey (02/11/2017) (364 days, Model 6–1) was significant over 69% of the area. Positive topographic change was present in 42% of the area above the $LoD_{95\%}$ while negative topographic change was dominant in extent (58%). The median negative topographic change rate was 71 mm, which was greater than the median positive topographic change rate (50 mm). Zones of intense negative topographic change were observed on the hillslopes, while there was a clear zone of deposition visible along the main drainage lines (Figure 3 (f)).

Two example transects were examined over the catchment where topographic changes were significant. Figure 4 shows the vertical difference between a series of surface elevation profiles across the profile AA' and BB'. For profile AA' the elevation was initially high at approximately 2.0 m, 3.1–4.0 m and 9.5 m distance along the profile on 04/11/2016 (Figure 4 (a), grey line), however, these sections experienced pronounced negative topographic changes during the subsequent field surveys. The maximum vertical displacement was about 500 mm at 3.2 m along the transect. For the sections between 0 and 1.8 m and 4.0 and 5.5 m along the transect, the surface elevation surveyed on 04/11/2016 was significantly lower than for the later surveys, indicating positive topographic changes occurred after the first field survey. For profile

BB', there was significant surface lowering at a distance 9.0 to 10.0 m along the transect with a maximum vertical displacement of ~700 mm. The survey on 13/06/2017 recorded surface elevation significantly higher at 5.0–7.0 m along the transect than those of the other surveys.

< Figure 4 is here >

Sediment production measured by sediment traps

Loss measured by sediment traps on the tributaries

Over the 10-month period of sediment trap observation, they captured 30.75 kg of peat (oven-dry weight). The sediment trapped during the intervals 13/06/2017–21/08/2017, 04/11/2016–23/03/2017 and 23/03/2017–07/04/2017 were 10.71 kg, 9.60 kg and 8.53 kg, respectively (Table 3). In contrast, the sediment trapped between 07/04/2017 and 13/06/2017 was significantly lower ($p < 0.05$) than for other survey periods, with a value of 1.91 kg. Among the six sediment traps T3 and T5 generally collected more sediment than other traps (Table 3), indicating that source areas of T3 and T5 were more actively eroding.

< Table 3 is here >

Over the full monitoring period T3 had the highest peat loss rate of 0.6 g m^{-2} d^{-1}, followed by T6 (0.5 g m^{-2} d^{-1}) and T1 (0.4 g m^{-2} d^{-1}) (Table 3). The total sediment captured by T2 was lowest, with 0.1 g m^{-2} d^{-1}. Among the different monitoring periods the interval 23/03/2017–07/04/2017 had the highest peat loss rate; while 07/04/2017 to 13/06/2017 had the smallest peat losses (Table 3).

Comparing SfM and sediment trap data

The sediment trap data allowed a comparison of ground recession to be made with SfM measurements. The peat loss data, expressed in kilograms and surface change (mm), derived from both the sediment traps and SfM is shown in Figure 5. The peat loss (dry weight) rate measured by the sediment traps ranged from 0.0 kg to 4.7 kg, with a mean value of 1.8 kg (standard error of mean is 0.3 kg) however this does not take into account any deposition that may take place. In contrast, the SfM measurements indicated both positive and negative values, allowing not only areas of erosion and deposition to be identified but also periods of time. At the catchment scale, the SfM method resulted in an estimated mean peat deposition rate of 93.3 ± 55.5 kg (5.3 ± 5.2 mm), compared with a mean peat loss rate of 1.8 ± 0.3 kg (0.3 ± 0.1 mm) derived from the sediment traps across the catchment (Figure 5). From the M3C2 distances and histogram of differences (Figure 3), there were both erosional and depositional areas within the catchment and these features were captured by SfM.

< Figure 5 is here >

Stream discharge and suspended sediment loads

Empirical suspended sediment-transport rating curves

A power law ($Q_s = aQ^b$) performed well in describing the relationship between suspended sediment yield (Q_s) and discharge (Q). However, the sediment rating curves differed between different months (Figure 6). High uncertainty with a low coefficient of determination (R^2) of the regression equations was found from February to June 2017. The values of coefficients *a* and *b*, which indicate erodibility and erosive power of flow respectively, varied considerably among different months. The

386 regression curve for the whole study period was $Q_s = 49505Q^{1.0441}$ (n = 176, R^2 =
387 0.6817, $p < 0.05$).
388 < Figure 6 is here >
389
390 Stream discharge and suspended sediment (SS) loads
391 Mean daily stream discharge estimated by the rainfall-runoff relationship for the 12-
392 month monitoring period was 0.0013 $m^3 s^{-1}$ (Table 4). Flows ranged over two orders
393 of magnitude, with a minimum mean discharge of 0.0001 $m^3 s^{-1}$ and a maximum mean
394 discharge of 0.0021 $m^3 s^{-1}$. There were 53 days when discharge exceeded 0.0021 m^3
395 s^{-1} during the study period (Figure 7). The majority of high flows occurred in the autumn
396 months (September and October) and early spring 2017 (March).
397 Suspended sediment (SS) loads ranged from 0.002 to 6.236 t with a total value of
398 14.822 t (Table 4). Despite some breaks in the record, some seasonal patterns can
399 be identified. Both SS and POC loads were low during late spring months (April and
400 May) and increased in the late summer and autumn and were highest in October. For
401 most of April to June 2017, discharge was maintained at a low level and very little
402 sediment was transported to the catchment outlet. However, there were two high flow
403 events (daily mean discharge rate > 0.006 $m^3 s^{-1}$) in late May and June which
404 mobilised a considerable amount of sediment (Figure 7).
405 < Table 4 is here >
406 < Figure 7 is here >
407
408 Particulate organic carbon loads
409 The relationship between POC load (Q_{POC}) and discharge (Q) was well described by
410 a power law ($Q_{POC} = aQ^b$) (Figure 8). Similar to the SS rating curves, the POC rating

411 curves had high uncertainty from February to June 2017. The values of coefficients *a*
412 and *b* varied significantly among different months. The regression curve for the whole
413 study period was $Q_{POC} = 15776Q^{1.0061}$ (n = 144, R^2 = 0.6245, $p < 0.05$). POC loss
414 ranged from 0.000 to 2.444 t per month, and the total POC flux was 5.454 t which
415 accounted for 36.8% of the total suspended sediment load.

416 < Figure 8 is here >

417

418 Scale effect of sediment production in headwater peatlands

419 The relationship between sediment yield and area is shown in Figure 9 also illustrating
420 which data were derived from the different approaches at the study site. At the fine
421 scale with area ranging from 1×10^{-5} to 1×10^{-3} km^2, sediment yield generally
422 decreased with increasing area. Spearman's Rank correlations between sediment
423 yield and area showed that the relationship was significant at p = 0.052 at the fine
424 scale (i.e. only marginally beyond a standard 95 % confidence level). The sediment
425 yield at the outlet of the whole study area was highest. Spearman's Rank correlations
426 between the sediment yield and area showed that the relationship was not significant
427 (p = 0.693).

428 < Figure 9 is here >

429

430 Discussion

431 Temporal evolution of eroding headwater peatlands

432 The study winter (Dec/Jan/Feb) had a mean temperature of 2.3 ºC. For northern
433 England the MetOffice (2018) reported that the study winter was warmer than the
434 1981-2010 mean for winter. A total of 55 freezing days occurred between 26/10/2016
435 and 07/04/2017. Diurnal freezing was common in November 2016 with temperature

436 frequently fluctuating above and below zero and needle ice was formed (Figure 10 (a)),
437 causing expansion of the peat surface. The large amount of peat material captured by
438 the sediment traps during the period 23/03/2017–07/04/2017, compared to the rest of
439 the study period, may have been related to a period of heavy rainfall from 30 to 31
440 March which occurred on the peat surface preconditioned by freeze–thaw weathering.
441 During the dry period from April to May 2017, hillslope peat exhibited substantial
442 desiccation (Figure 10 (b)). Surface desiccation also affected deposited peat within
443 the river channels and overbank areas. Field observations showed that on the
444 desiccated peat surface the upper dried crust was generally concave in shape and
445 detached from the intact peat below, a feature also reported by Evans and Warburton
446 (2007). Cracks often connected in the form of polygons and were up to 12 cm deep.
447 The peat loss rate measured by sediment traps during the period of 07/04/2017–
448 13/06/2017 was the lowest during the study due to low rainfall (Table 3). However, the
449 sediment trapped during the subsequent period with higher rainfall totals (13/06/2017–
450 21/08/2017) was the highest observed (Table 3). These results are in agreement with
451 those reported in other blanket peatland environments, surface desiccation during
452 extended periods of dry weather has been shown to be an important weathering
453 process for producing erodible peat (Burt and Gardiner, 1984, Evans et al., 1999,
454 Francis, 1990, Holden and Burt, 2002). Similar seasonal patterns of sediment capture
455 have also been reported by Francis (1990) and Labadz et al. (1991) who found little
456 peat sediment removed during the summer or late winter/spring, with the majority
457 captured in the autumn and early winter.

458 < Figure 10 is here >

459

Scale effect of sediment production in headwater peatlands

Peat erosion decreased with increasing area at the fine scale for areas less than 1 × 10^{-3} km^2 (Figure 9) where erosion processes are dominated by rill and interrill erosion (Li et al., 2018a). This scale effect on peat erosion values could be explained by decreasing sediment delivery ratios with increasing area (Walling and Webb, 1996). The fact that sediment yield was highest for the whole study area (0.017 km^2) suggests that gully erosion, channel bank erosion and flushing of deposited materials could be important sediment sources at larger scales. A number of previous studies have shown that bank erosion (Small et al., 2003), gully erosion and mass movements (Evans and Warburton, 2007, Evans et al., 2006) form an important part of the catchment sediment budget in upland peat catchments. At larger scales erosion and transport of mineral materials might become even more important, with mineral sediment accounting for 63.2% of the total sediment yield at Fleet Moss. Mineral sediments in these upland systems may be loosened and mobilized in different ways and may not require freeze-thaw and desiccation to make them available for transport.

This study has shown that peat loss measurements at one scale are not representative of sediment yield at another scale level. Therefore, direct extrapolation of plot scale interrill and rill erosion rates up the catchment scale can be problematic. Different erosion processes are active at different spatial scales, and different sediment sinks and sources appear from plot to catchment scale (Li, 2019). More monitoring, experimental and modelling studies are needed as a basis for scaling erosion rates from one specific area to larger or smaller areas. In addition, it is suggested that monitoring of peat erosion processes should utilize standardized procedures to allow comparisons of data obtained from different study areas.

Sediment production estimated from topographic change measured by SfM and sediment traps

The error obtained during the manual registration of the SfM point clouds (mean value of 41 mm) (Table 1) is within the range of registration errors (i.e. 11–291 mm, mean 46 mm) found in a previous study in natural terrain (Glendell et al., 2017). Although both positive and negative net topographic changes were observed over different survey intervals, the net topographic change observed over the whole monitoring period was –27 mm (Table 2). This value is in agreement with data from other UK sites where topographic change rates (-24 ± 8 mm yr^{-1}) were measured using erosion pins (Evans and Warburton, 2007, Grayson et al., 2012); and those (–286 mm to +31 mm yr^{-1}; mean value of –33 mm yr^{-1}) measured using SfM (Glendell et al., 2017).

Peat erosion measurement using sediment traps and SfM have different applications. For many applications mass loss captured by sediment traps or estimated by river sediment yield studies is a key parameter of interest; while for other applications surface change is used as a proxy for erosion. It should be noted from mass balance principles that all things being equal, the estimates of mass loss using different methods should be comparable. However, in this study peat loss data estimated from the sediment traps and SfM techniques did not match well with each other (Figure 5). Deposition-related change measured by SfM was 93.3 ± 55.5 kg (5.3 ± 5.2 mm), in comparison with erosion-related change derived from the sediment traps of 1.8 ± 0.3 kg (0.3 ± 0.1 mm). The discrepancy could be explained by two reasons. The first explanation is associated with wind erosion, oxidation loss of the peat and shrinkage of the peat by compression that can cause topographic change captured by SfM but not by sediment traps. For example, 30–81% of surface lowering has previously been attributed to peat wastage in upland peat environments (Francis, 1990,

Evans and Warburton, 2007, Evans et al., 2006) though it is thought that this estimate probably includes both oxidation loss (i.e. true wastage) and compression of the peat associated with loss of water and collapse of the pore structure leading to higher bulk density values. In addition, eroded peat is loose and less compact than when it was *in situ* and so re-deposition of such loose peat materials could result in positive topographic change which is well captured by SfM. However, such changes to peat bulk density would not often be accounted for in stream sediment sampling or sediment trap data which examines dry mass loss.

Loss of organic sediment from the catchment

The estimated annual total suspended sediment load leaving the catchment was calculated as 14.8 tonnes per year, equivalent to 926.3 t km^{-2} yr^{-1}. This value at Fleet Moss is much greater than those reported from other upland blanket peatlands (generally less than 200 t km^{-2} yr^{-1}, cited in Li et al. (2018a)). The estimated POC load was 5.5 t yr^{-1}, equivalent to 340.9 t organic carbon km^{-2} yr^{-1} and accounted for 36.8% of the total suspended sediment load. The POC flux is greater than those reported (0.12–38.9 t C km^{-2} yr^{-1}) in other peatland catchments in the UK (Francis, 1990, Labadz et al., 1991, Hutchinson, 1995, Dawson et al., 2002, Dawson et al., 1995, Holden, 2006, Worrall et al., 2003). It is recognised that the discharge from the catchment was not continuously gauged due to instrument errors and that continuous gauging combined with storm event sediment sampling would improve the stream sediment flux estimates for Fleet Moss. In this study, daily stream sampling for sediment concentrations was used but this technique may miss important sediment transport events such as storms, which could be important as peat systems often have flashy regimes. Sediment concentration-discharge hysteresis can occur during events

meaning that the sediment-discharge rating equation can vary (Li et al., 2018a). Thus our estimates of catchment sediment yield are approximate. Nevertheless, the evidence presented using multiple data sources suggests that there is a very high erosion and organic carbon loss rate from the system and high localized rates of topographic change measured in only 12 months (i.e. 500–700 mm in some places). Thus Fleet Moss is rapidly eroding, exporting large amounts of sediment and particulate carbon and could be a hot spot target for restoration intervention to stabilize the peatland and reduce future erosion.

Conclusions

The net topographic change for the studied catchment within Fleet Moss derived from SfM was negative during the 12-month monitoring period. A comparison of topographic changes for a series of nested small watersheds derived from SfM and sediment traps showed significant differences with a positive topographic change determined by the SfM and a negative topographic change from the sediment traps. This difference indicates that it is problematic to directly interpolate peat erosion rates measured by local net topographic change that can be as high as 500–700 mm into sediment yield at the catchment outlet, without considering sediment sinks within the catchment budget. Desiccation and freeze–thaw processes were identified as playing key roles in breaking up the peat surface prior to removal by fluvial processes. The greatest sediment and organic carbon losses occurred during the autumn following a two-month period of dry weather in spring during which desiccation was observed and summer period when bare peat was exposed to warmer weather and more desiccation. Frost action played an important role in providing available sediment during the winter months via needle-ice formation and thaw. Peat loss measured at the hillslope scale

was not representative of that at catchment scale within which bank erosion, mass movements and transport of eroded mineral sediment could also be important.

Acknowledgements

The work was jointly funded by the China Scholarship Council and the University of Leeds (File No. 201406040068). Jonathan Carrivick and Lee Brown are thanked for providing the Geodimeter and tinytag temperature loggers used in this study. Special acknowledgement is given to David Ashley who helped prepare the laboratory experimental materials and field set-up. Santiago Clerici and Sarah Hunt are much acknowledged for their time and assistance involved in field work. Mark Smith, Duncan Quincey, Scott Watson and Joe Mallalieu are thanked for providing advice on using Agisoft Photoscan and Cloudcompare to undertake data analysis. Guidance by Josh Greenwood for water sample (POC) analysis is acknowledged. We are grateful to Claudio Bravo L. for providing help in data visualization. Jeff Warburton (Department of Geography, Durham University) is thanked for sharing experience and providing advice for the design of sediment traps.

References

BALL, D. 1964. Loss - on - ignition as an estimate of organic matter and organic carbon in non - calcareous soils. *Journal of soil science,* 15**,** 84-92.

BAYNES, E. R. C. 2012. *Peat bog restoration: Implications of erosion and sediment transfer at Flow Moss, North Pennines.* Durham thesis, Durham University.

BILLETT, M., CHARMAN, D., CLARK, J., EVANS, C., EVANS, M., OSTLE, N., WORRALL, F., BURDEN, A., DINSMORE, K. & JONES, T. 2010. Carbon balance of UK peatlands: current state of knowledge and future research challenges. *Climate Research,* 45**,** 13-29.

BONN, A., ALLOTT, T., HUBACEK, K. & STEWART, J. 2009. *Drivers of environmental change in uplands*, Routledge.

BOWER, M. 1960a. The erosion of blanket peat in the southern Pennines. *East Midland Geographer,* 13**,** 22-33.

BOWER, M. 1960b. Peat erosion in the Pennines. *Advancement of Science,* 64**,** 323-331.

BOWER, M. 1961. The distribution of erosion in blanket peat bogs in the Pennines. *Transactions and Papers (Institute of British Geographers),* 29**,** 17-30.

BURT, T. & GARDINER, A. 1984. Runoff and sediment production in a small peat-covered catchment: some preliminary results. *Catchment Experiments in Fluvial Geomorphology* Norwich, England: Geo Books.

CANNELL, M., DEWAR, R. & PYATT, D. 1993. Conifer plantations on drained peatlands in Britain: a net gain or loss of carbon? *Forestry: An International Journal of Forest Research,* 66**,** 353-369.

CLAY, G. D., DIXON, S., EVANS, M. G., ROWSON, J. G. & WORRALL, F. 2012. Carbon dioxide fluxes and DOC concentrations of eroding blanket peat gullies. *Earth Surface Processes and Landforms,* 37**,** 562-571.

CRISP, D. 1966. Input and output of minerals for an area of Pennine moorland: the importance of precipitation, drainage, peat erosion and animals. *Journal of Applied Ecology,* 3**,** 327-348.

DAWSON, J., BILLETT, M., NEAL, C. & HILL, S. 2002. A comparison of particulate, dissolved and gaseous carbon in two contrasting upland streams in the UK. *Journal of Hydrology,* 257**,** 226-246.

DAWSON, J., HOPE, D., CRESSER, M. & BILLETT, M. 1995. Downstream changes in free carbon dioxide in an upland catchment from northeastern Scotland. *Journal of Environmental Quality,* 24**,** 699-706.

DE VENTE, J. & POESEN, J. 2005. Predicting soil erosion and sediment yield at the basin scale: Scale issues and semi-quantitative models. *Earth-Science Reviews,* 71**,** 95-125.

EVANS, M., BURT, T., HOLDEN, J. & ADAMSON, J. 1999. Runoff generation and water table fluctuations in blanket peat: evidence from UK data spanning the dry summer of 1995. *Journal of Hydrology,* 221**,** 141-160.

EVANS, M. & LINDSAY, J. 2010. Impact of gully erosion on carbon sequestration in blanket peatlands. *Climate Research,* 45**,** 31-41.

EVANS, M. & WARBURTON, J. 2005. Sediment budget for an eroding peat - moorland catchment in northern England. *Earth Surface Processes and Landforms,* 30**,** 557-577.

EVANS, M. & WARBURTON, J. 2007. *Geomorphology of upland peat: erosion, form and landscape change,* Oxford, UK, John Wiley & Sons.

EVANS, M., WARBURTON, J. & YANG, J. 2006. Eroding blanket peat catchments: global and local implications of upland organic sediment budgets. *Geomorphology,* 79**,** 45-57.

FEWINGS, R. 2014. *Assessing the Impact of Peat Bog Restoration in Mitigating Carbon Loss by Upland Erosion.* Doctoral dissertation, Durham University.

FONSTAD, M. A., DIETRICH, J. T., COURVILLE, B. C., JENSEN, J. L. & CARBONNEAU, P. E. 2013. Topographic structure from motion: a new development in photogrammetric measurement. *Earth Surface Processes and Landforms,* 38**,** 421-430.

FRANCIS, I. 1990. Blanket peat erosion in a mid ‐ wales catchment during two drought years. *Earth Surface Processes and Landforms,* 15**,** 445-456.

GLENDELL, M., MCSHANE, G., FARROW, L., JAMES, M. R., QUINTON, J., ANDERSON, K., EVANS, M., BENAUD, P., RAWLINS, B. & MORGAN, D. 2017. Testing the utility of structure ‐ from ‐ motion photogrammetry reconstructions using small unmanned aerial vehicles and ground photography to estimate the extent of upland soil erosion. *Earth Surface Processes and Landforms,* 42**,** 1860-1871.

GOULSBRA, C. S., EVANS, M. G. & ALLOTT, T. E. J. A. S. 2016. Rates of CO 2 efflux and changes in DOC concentration resulting from the addition of POC to the fluvial system in peatlands. 78**,** 477-489.

GRAB, S. W. & DESCHAMPS, C. L. 2004. Geomorphological and geoecological controls and processes following gully development in alpine mires, Lesotho. *Arctic, Antarctic, and Alpine Research,* 36**,** 49-58.

GRAYSON, R., HOLDEN, J., JONES, R., CARLE, J. & LLOYD, A. 2012. Improving particulate carbon loss estimates in eroding peatlands through the use of terrestrial laser scanning. *Geomorphology,* 179**,** 240-248.

HOLDEN, J. 2006. Sediment and particulate carbon removal by pipe erosion increase over time in blanket peatlands as a consequence of land drainage. *Journal of Geophysical Research: Earth Surface (2003–2012),* 111.

HOLDEN, J. & BURT, T. 2002. Infiltration, runoff and sediment production in blanket peat catchments: implications of field rainfall simulation experiments. *Hydrological Processes,* 16**,** 2537-2557.

HOLDEN, J., GREEN, S. M., BAIRD, A. J., GRAYSON, R. P., DOOLING, G. P., CHAPMAN, P. J., EVANS, C. D., PEACOCK, M. & SWINDLES, G. 2017. The impact of ditch blocking on the hydrological functioning of blanket peatlands. *Hydrological processes,* 31**,** 525-539.

HOLDEN, J., KIRKBY, M. J., LANE, S. N., MILLEDGE, D. G., BROOKES, C. J., HOLDEN, V. & MCDONALD, A. T. 2008. Overland flow velocity and roughness properties in peatlands. *Water Resources Research,* 44**,** W06415.

HOLDEN, J., SHOTBOLT, L., BONN, A., BURT, T., CHAPMAN, P., DOUGILL, A., FRASER, E., HUBACEK, K., IRVINE, B. & KIRKBY, M. 2007. Environmental change in moorland landscapes. *Earth-Science Reviews,* 82**,** 75-100.

HOLDEN, J., SMART, R. P., DINSMORE, K. J., BAIRD, A. J., BILLETT, M. F. & CHAPMAN, P. J. 2012. Natural pipes in blanket peatlands: major point sources for the release of carbon to the aquatic system. *Global Change Biology,* 18**,** 3568-3580.

HOPE, D., BILLETT, M. F., MILNE, R. & BROWN, T. A. 1997. Exports of organic carbon in British rivers. *Hydrological Processes,* 11**,** 325-344.

HUTCHINSON, S. M. 1995. Use of magnetic and radiometric measurements to investigate erosion and sedimentation in a British upland catchment. *Earth Surface Processes and Landforms,* 20**,** 293-314.

LABADZ, J., BURT, T. & POTTER, A. 1991. Sediment yield and delivery in the blanket peat moorlands of the Southern Pennines. *Earth Surface Processes and Landforms,* 16**,** 255-271.

LAGUE, D., BRODU, N. & LEROUX, J. 2013. Accurate 3D comparison of complex topography with terrestrial laser scanner: Application to the Rangitikei canyon (NZ). *ISPRS Journal of Photogrammetry and Remote Sensing,* 82**,** 10-26.

LI, C. 2019. *Peat erosion: processes, patterns and rates.* Doctoral dissertation, University of Leeds.

LI, C., GRAYSON, R., HOLDEN, J. & LI, P. 2018a. Erosion in peatlands: Recent research progress and future directions. *Earth-Science Reviews,* 185**,** 870-886.

LI, C., GRAYSON, R., SMITH, M. & HOLDEN, J. 2019. Patterns and drivers of peat erosion via using Structure-from-Motion photogrammetry at field plot and laboratory scales. *Earth Surface Processes and Landforms*.

LI, C., HOLDEN, J. & GRAYSON, R. 2018b. Effects of needle ice production and thaw on peat erosion processes during overland flow events. *Journal of Geophysical Research: Earth Surface,* 123**,** 2107-2122

LI, C., HOLDEN, J. & GRAYSON, R. 2018c. Effects of rainfall, overland flow and their interactions on peatland interrill erosion processes. *Earth Surface Processes and Landforms,* 43**,** 1451-1464.

LI, P., HOLDEN, J. & IRVINE, B. 2016a. Prediction of blanket peat erosion across Great Britain under environmental change. *Climatic Change,* 134**,** 177-191.

LI, P., HOLDEN, J., IRVINE, B. & GRAYSON, R. 2016b. PESERA‐PEAT: a fluvial erosion model for blanket peatlands. *Earth Surface Processes and Landforms,* 41**,** 2058-2077.

LI, P., HOLDEN, J., IRVINE, B. & MU, X. 2017. Erosion of Northern Hemisphere blanket peatlands under 21st‐century climate change. *Geophysical Research Letters,* 44**,** 3615-3623.

LUOTO, M. & SEPPäLä, M. 2000. Summit peats ('peat cakes') on the fells of Finnish Lapland: continental fragments of blanket mires? *The Holocene,* 10**,** 229-241.

MARC, V. & ROBINSON, M. 2007. The long-term water balance (1972-2004) of upland forestry and grassland at Plynlimon, mid-Wales. *Hydrology and Earth System Sciences,* 11**,** 44-60.

METOFFICE 2018. Maps of climate variables for months, seasons and years https://www.metoffice.gov.uk/climate/uk/summaries/anomacts.

MILNE, R. & BROWN, T. 1997. Carbon in the vegetation and soils of Great Britain. *Journal of Environmental Management,* 49**,** 413-433.

PARRY, L. E., HOLDEN, J. & CHAPMAN, P. J. 2014. Restoration of blanket peatlands. *Journal of Environmental Management,* 133**,** 193-205.

PAWSON, R., EVANS, M. & ALLOTT, T. 2012. Fluvial carbon flux from headwater peatland streams: significance of particulate carbon flux. *Earth Surface Processes and Landforms,* 37**,** 1203-1212.

PAWSON, R., LORD, D., EVANS, M. & ALLOTT, T. 2008. Fluvial organic carbon flux from an eroding peatland catchment, southern Pennines, UK. *Hydrology and Earth System Sciences,* 12**,** 625-634.

SHUTTLEWORTH, E., EVANS, M., HUTCHINSON, S. & ROTHWELL, J. 2015. Peatland restoration: controls on sediment production and reductions in carbon and pollutant export. *Earth Surface Processes and Landforms,* 40**,** 459-472.

SHUTTLEWORTH, E. L., CLAY, G. D., EVANS, M. G., HUTCHINSON, S. M. & ROTHWELL, J. J. 2017. Contaminated sediment dynamics in peatland headwater catchments. *Journal of Soils and Sediments,* 17**,** 1-11.

SMALL, I., ROWAN, J. & DUCK, R. 2003. Long-term sediment yield in Crombie Reservoir catchment, Angus; and its regional significance within the Midland Valley of Scotland. *Hydrological Sciences Journal,* 48**,** 619-635.

SMITH, M., CARRIVICK, J., HOOKE, J. & KIRKBY, M. 2014. Reconstructing flash flood magnitudes using 'Structure-from-Motion': A rapid assessment tool. *Journal of Hydrology,* 519**,** 1914-1927.

SNAPIR, B., HOBBS, S. & WAINE, T. 2014. Roughness measurements over an agricultural soil surface with Structure from Motion. *ISPRS Journal of Photogrammetry and Remote Sensing,* 96**,** 210-223.

STIMSON, A. G. 2016. *Fluvial carbon dynamics in degraded peatland catchments.* The University of Manchester (United Kingdom).

STöCKER, C., ELTNER, A. & KARRASCH, P. 2015. Measuring gullies by synergetic application of UAV and close range photogrammetry—A case study from Andalusia, Spain. *Catena,* 132**,** 1-11.

TALLIS, J. 1973. Studies on southern Pennine peats: V. Direct observations on peat erosion and peat hydrology at Featherbed Moss, Derbyshire. *The Journal of Ecology,* 61**,** 1-22.

WALLING, D. E. & WEBB, B. 1996. *Erosion and Sediment Yield: Global and Regional Perspectives: Proceedings of an International Symposium Held at Exeter, UK, from 15 to 19 July 1996*, IAHS.

WESTOBY, M. J., DUNNING, S. A., HEIN, A. S., MARRERO, S. M. & SUGDEN, D. E. 2016. Interannual surface evolution of an Antarctic blue-ice moraine using multi-temporal DEMs. *Earth Surface Dynamics,* 4**,** 515.

WORRALL, F., BURT, T., ROWSON, J., WARBURTON, J. & ADAMSON, J. 2009. The multi-annual carbon budget of a peat-covered catchment. *Science of the Total Environment,* 407**,** 4084-4094.

WORRALL, F., REED, M., WARBURTON, J. & BURT, T. 2003. Carbon budget for a British upland peat catchment. *Science of the Total Environment,* 312**,** 133-146.

XU, J., MORRIS, P. J., LIU, J. & HOLDEN, J. 2018a. Hotspots of peatland-derived potable water use identified by global analysis. *Nature Sustainability,* 1**,** 246.

XU, J., MORRIS, P. J., LIU, J. & HOLDEN, J. 2018b. PEATMAP: Refining estimates of global peatland distribution based on a meta-analysis. *Catena,* 160**,** 134-140.

YU, Z., LOISEL, J., BROSSEAU, D. P., BEILMAN, D. W. & HUNT, S. J. 2010. Global peatland dynamics since the Last Glacial Maximum. *Geophysical Research Letters,* 37.

Tables

Table 1. Summary of georeferencing errors (i.e. RMSE on control points) for the field surveys.

Survey date	No. of images	No. of GCPs	Georeferencing RMSE (mm)
04/11/2016	197	6	43.9
02/05/2017	166	6	33.3
13/06/2017	104	6	42.8
21/08/2017	197	6	49.2
27/09/2017	165	6	37.1
02/11/2017	208	6	36.8

Table 2. Summary of the median net, positive and negative topographic changes (mm) with root mean square (RMS) (mm) for comparisons over different survey intervals. The long-term survey intervals are highlighted with bold.

Model[a]	Differencing epoch	Mean temperature (°C)	Rainfall (mm)	Net change			Positive change			Negative change		
				Median	RMS	Area (m^2 and %[b])	Median	RMS	Area (m^2 and %[c])	Median	RMS	Area (m^2 and %[**])
2–1	04/11/2016–02/05/2017	3.7	720.4	–18	85	414.3 (69%)	50	82	198.1 (48%)	–65	88	216.2 (52%)
3–2	02/05/2017–13/06/2017	11.2	225.4	–29	66	461.8 (77%)	46	71	229.8 (32%)	–43	64	349.3 (68%)
4–3	13/06/2017–21/08/2017	13.5	457.0	21	66	431.9 (72%)	39	65	299.0 (60%)	–41	69	243.4 (40%)
5–4	21/08/2017–27/09/2017	–	226.4	–21	62	438.5 (73%)	38	65	245.3 (40%)	–36	59	310.8 (60%)
6–5	27/09/2017–	–	396.4	24	64	433.6	40	64	300.8 (63%)	–40	63	232.8

	02/11/201					(73						(37%
	7					%)						)
6–	**04/11/201**	**–**	**1997.4**	**–**	**9**	**413**	**50**	**84**	**205.5**	**–**	**95**	**302.**
1	**6–**			**27**	**0**	**.3**			**(42%)**	**71**		**6**
	02/11/201					(69						**(58%**
	7					%)						**)**

[a] Model refers to difference between a survey of late date and a survey of earlier date.

[b] Percentage of the area above the $LoD_{95\%}$.

[c] Percentage of the area with significant changes.

Note: RMS is the square root of the arithmetic mean of the squares of a set of values.

Table 3. Summary of peat loss rates and net topographic change measured by sediment traps. '–' indicates not reported. Peat loss obtained from sediment traps was converted to an estimate of net topographic change using peat bulk density values from the study site.

Monitoring interval	Sediment traps	Peat loss rate (kg)	Peat loss (g m^{-2} d^{-1})	Net topographic change (mm)
04/11/2016–23/03/2017	T1	1.24	0.4	0.3
	T2	1.01	0.1	0.1
	T3	2.27	0.4	0.5
	T4	0.84	0.1	0.1
	T5	2.65	0.2	0.2
	T6	1.59	0.3	0.3
	Total	**9.60**		
23/03/2017–07/04/2017	T1	0.87	2.5	0.2
	T2	0.62	0.5	0.0
	T3	2.40	3.4	0.6
	T4	1.26	1.6	0.1
	T5	1.65	1.2	0.1
	T6	1.73	3.3	0.3
	Total	**8.53**		
07/04/2017–13/06/2017	T1	0.41	0.3	0.1
	T2	0.13	0.0	0.0
	T3	0.37	0.1	0.0
	T4	–	–	–
	T5	0.77	0.1	0.0
	T6	0.23	0.1	0.0
	Total	**1.91**		
13/06/2017–21/08/2017	T1	–	–	–
	T2	1.17	0.2	0.1
	T3	3.21	1.0	0.4
	T4	2.35	0.7	0.3
	T5	2.83	0.5	0.2
	T6	1.15	0.5	0.2
	Total	**10.71**		

Table 4. Summary of suspended sediment load and POC load during different months, seasons and whole monitoring period.

	Mean discharge (m^3 s^{-1})	SS load (t)	POC load (t)
November 2016	0.0006	0.069	-
December 2016	0.0006	0.204	-
January 2017	0.0005	0.150	-
February 2017	0.0011	0.323	0.114
March 2017	0.0012	0.592	0.194
April 2017	0.0001	0.002	0.000
May 2017	0.0005	0.002	0.000
June 2017	0.0014	1.100	0.400
July 2017	0.0012	2.237	0.838
August 2017	0.0009	1.475	0.550
September 2017	0.0012	2.431	0.912
October 2017	0.0021	6.236	2.444
Winter 2016	0.0009	0.677	0.114
Spring 2017	0.0008	0.596	0.195
Summer 2017	0.0017	4.813	1.788
Autumn 2017	0.0023	8.667	3.357
Whole monitoring period	0.0013	14.822	5.454

Figures

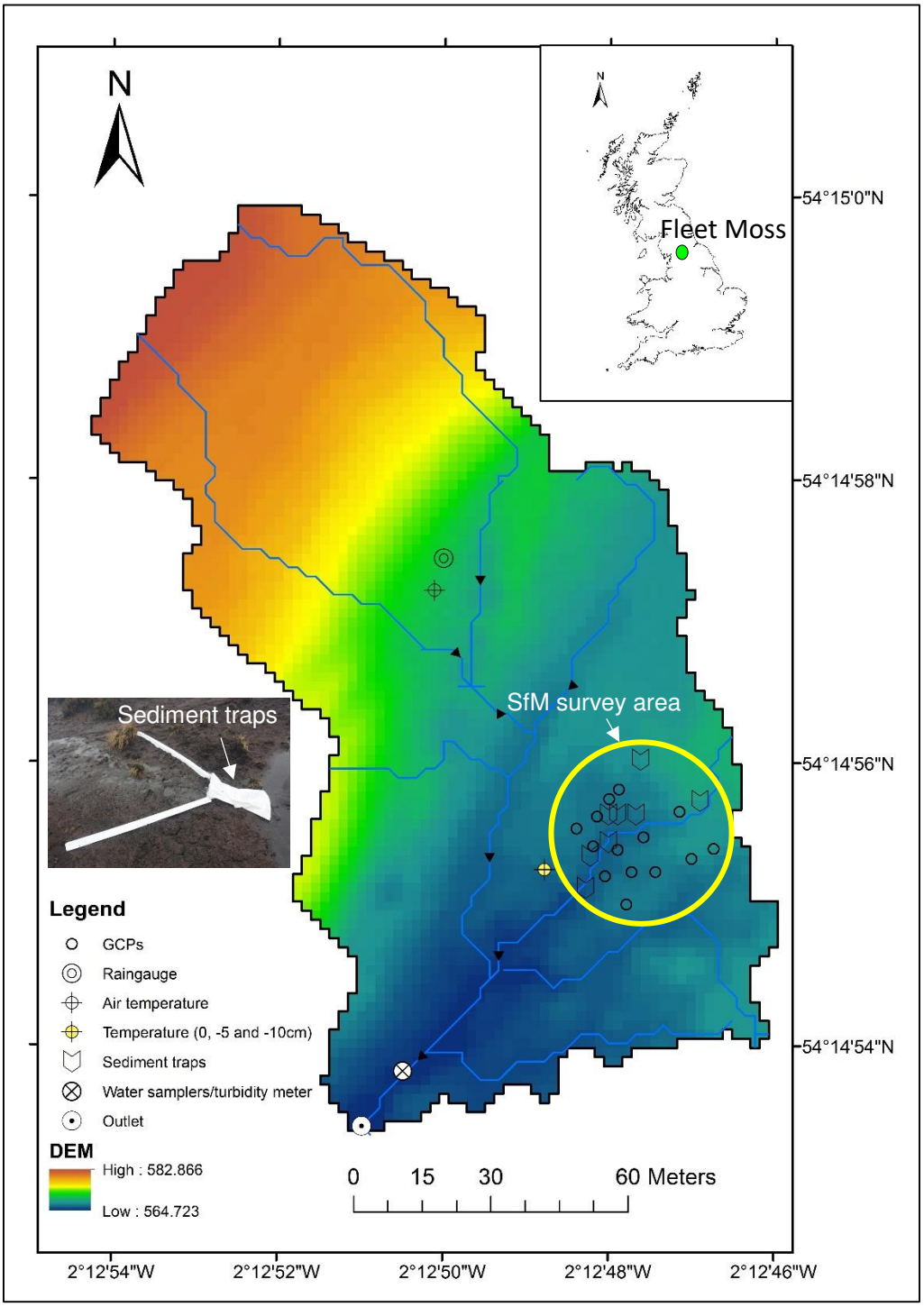

Figure 1. Map showing the position of Fleet Moss within the UK and the locations of field instruments in the research catchment (1.7 ha). Within the catchment there was a mini-catchment (990 m^2) where sediment traps were distributed and SfM surveys were conducted. An example sediment trap is shown in the inset photograph.

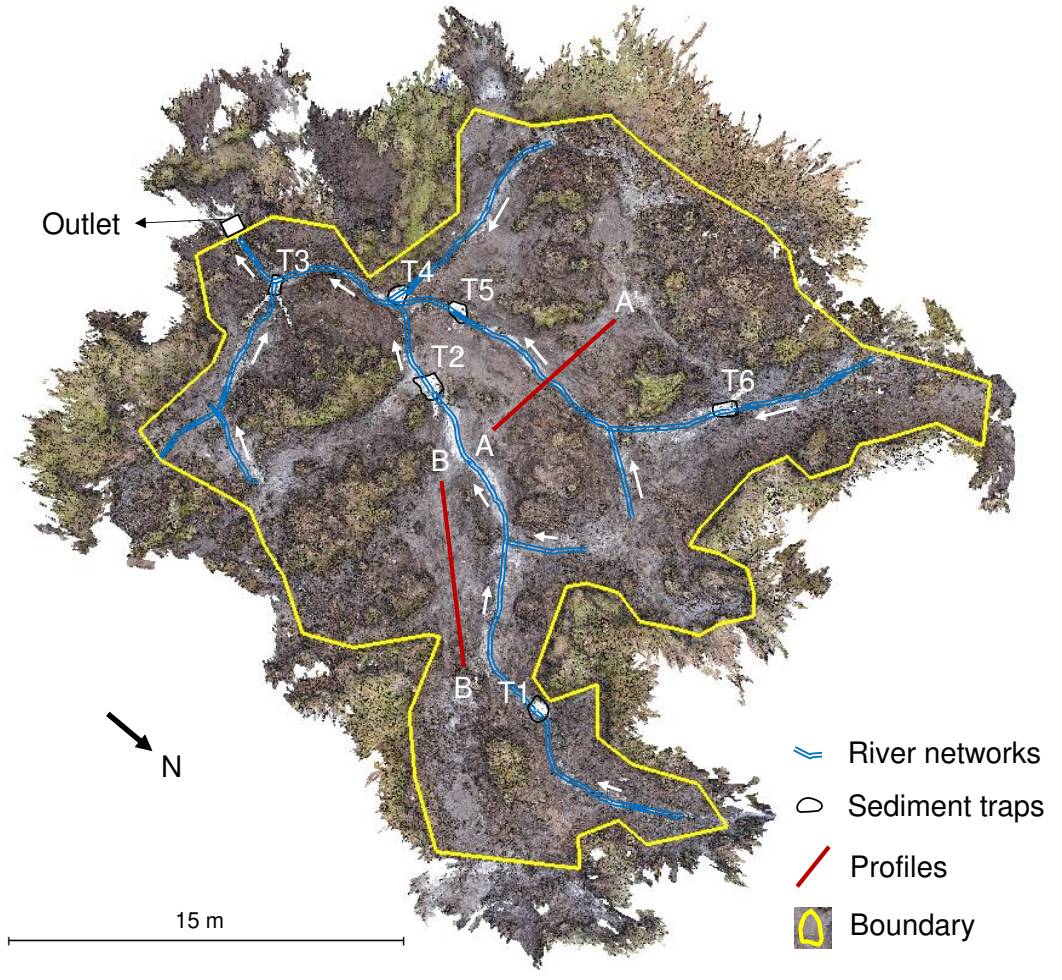

Figure 2. Orthophoto of the small-catchment (990 m^2) and the SfM focus area (with boundary outlined with yellow) (598 m^2). The sediment traps are numbered T1–T6. While the transect profiles are labelled A-A' and B-B' shown by the red lines.

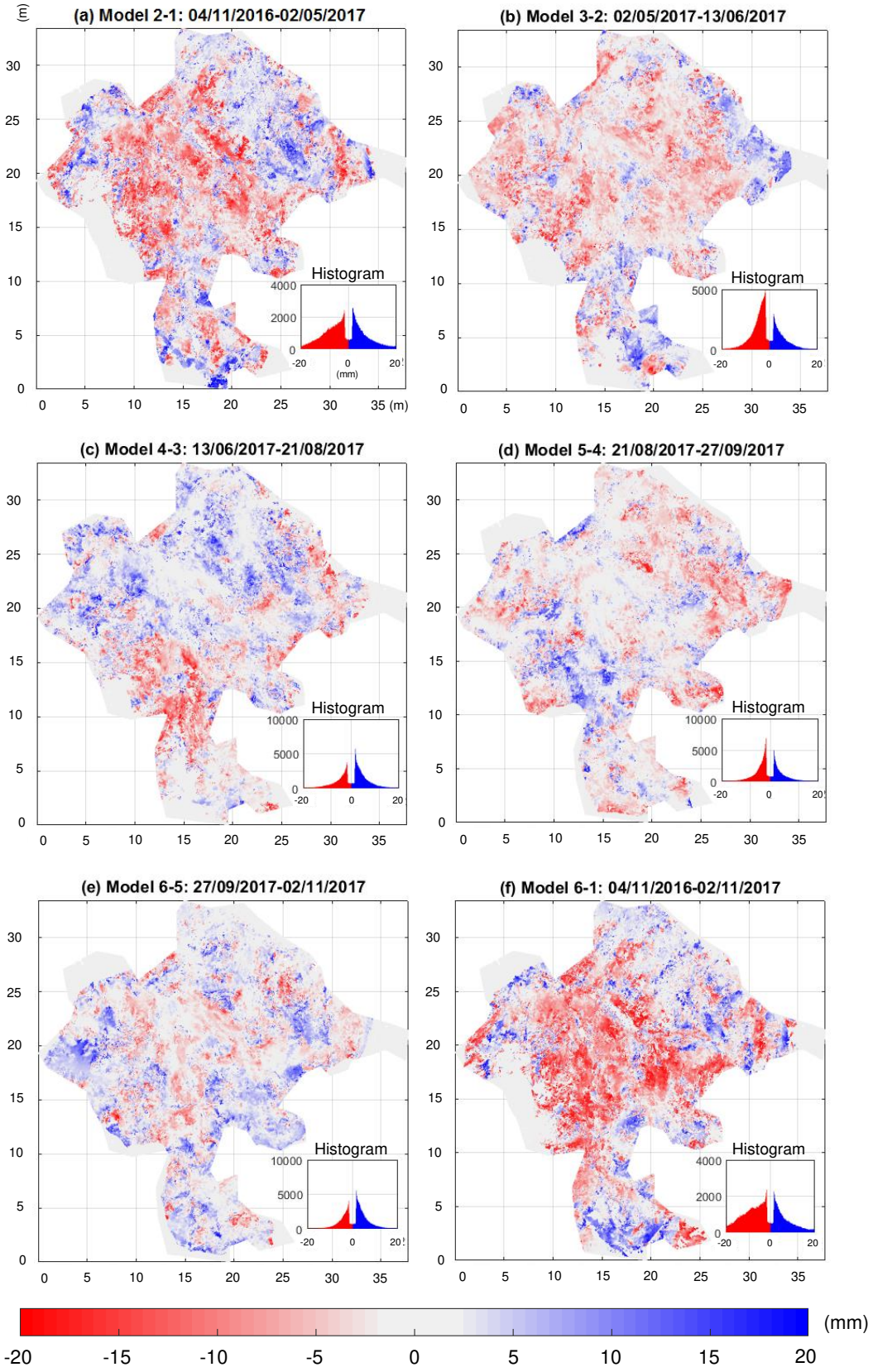
(a) Model 2-1: 04/11/2016-02/05/2017
(b) Model 3-2: 02/05/2017-13/06/2017
(c) Model 4-3: 13/06/2017-21/08/2017
(d) Model 5-4: 21/08/2017-27/09/2017
(e) Model 6-5: 27/09/2017-02/11/2017
(f) Model 6-1: 04/11/2016-02/11/2017
Histogram
(m)
(mm)
-20 -15 -10 -5 0 5 10 15 20

Figure 3. SfM determined M3C2 distances and histograms over different survey intervals (a–f) for the studied catchment. Grey areas have non-significant changes. Blue colours indicate positive topographic change and red colours show negative topographic change.

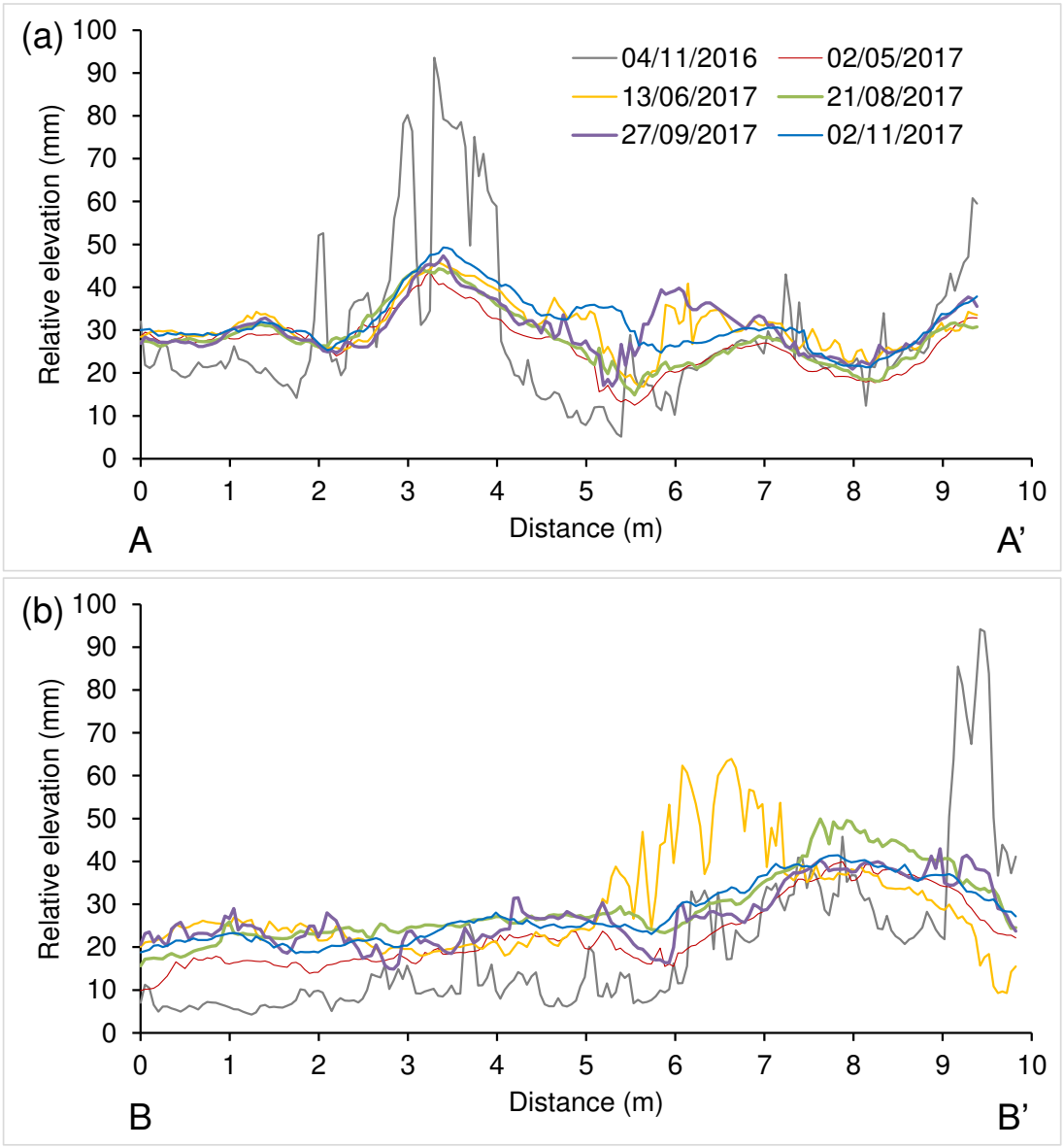

Figure 4. SfM measured 2-D peat profiles of (a) AA' and (b) BB' revealing topographic change over the monitored period. For the location of the cross-sections, see Figure 2.

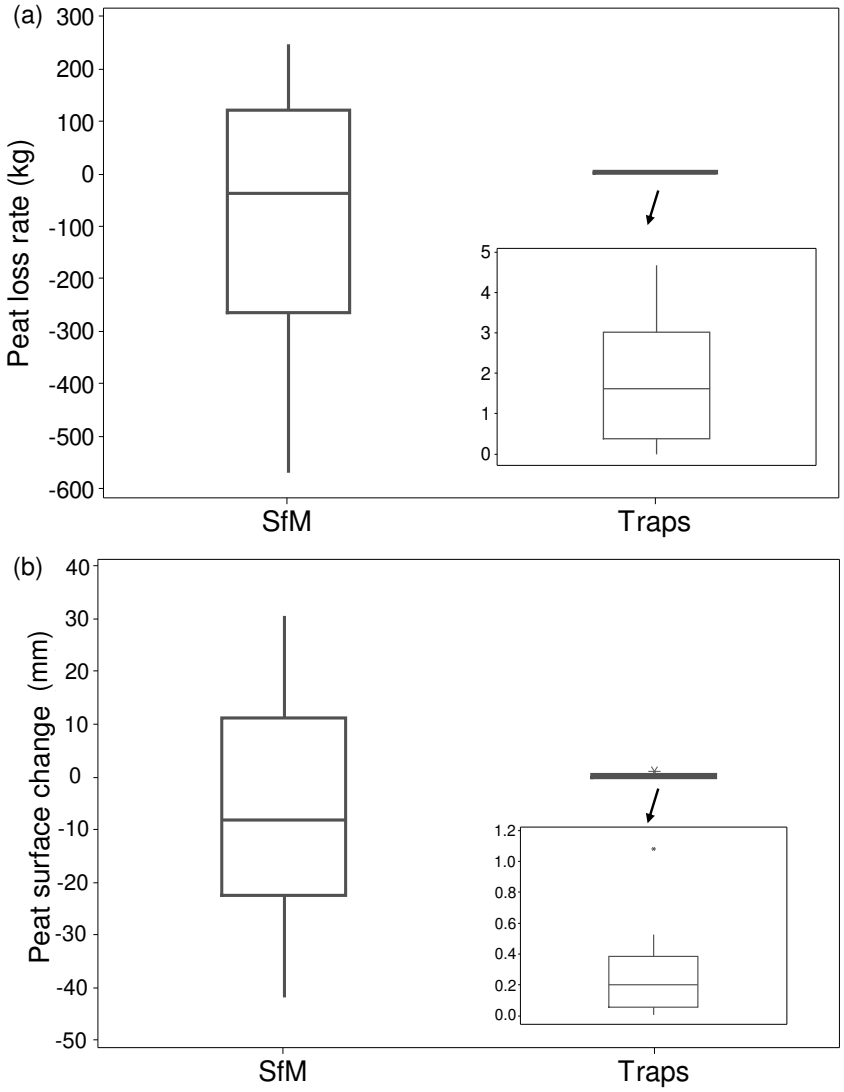

Figure 5. Summary of (a) peat loss (positive values show erosion; negative values show deposition) and (b) surface change (positive values show deposition; negative values show erosion) measured by SfM and sample trap methods.

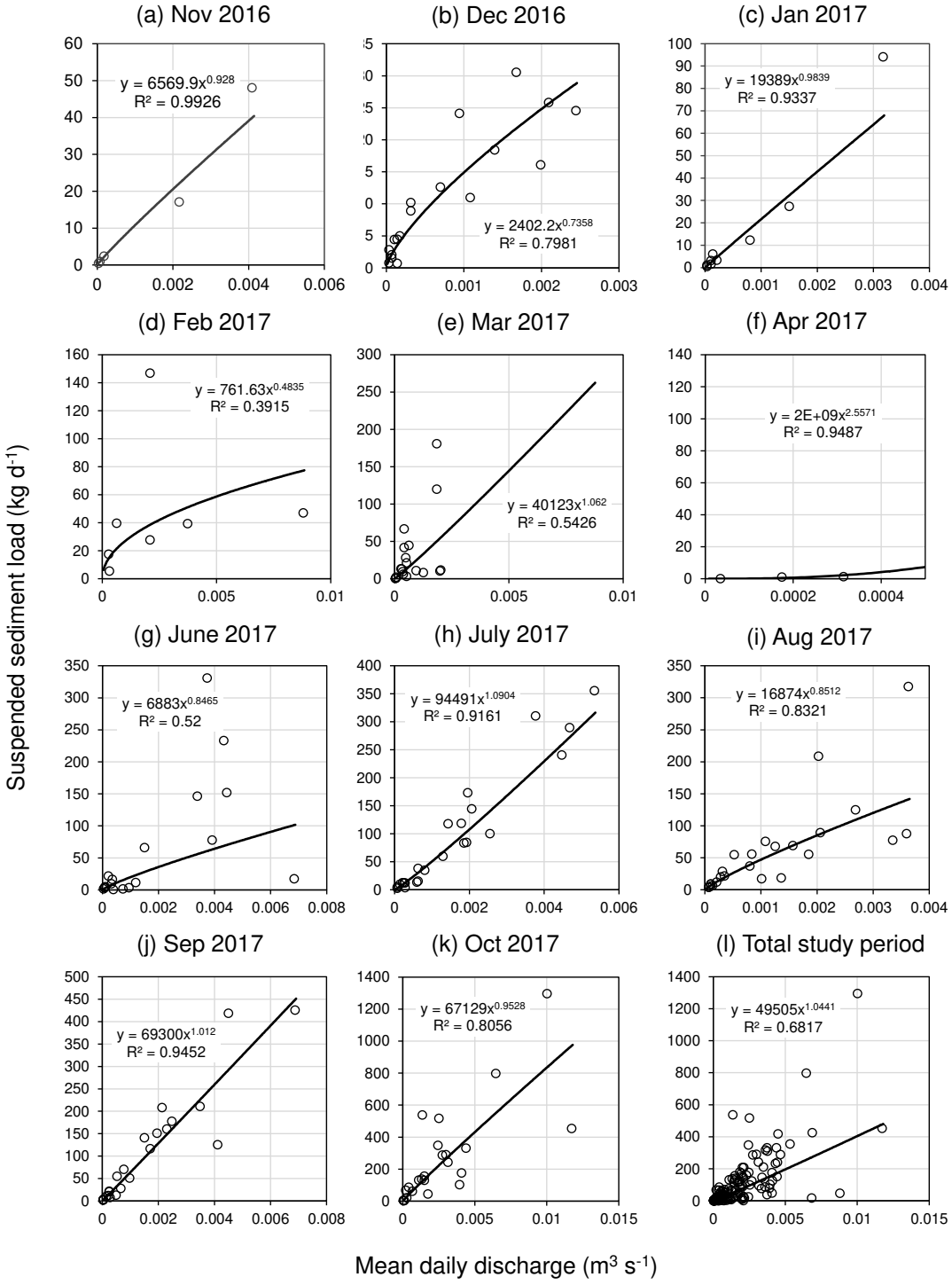

Figure 6. Stream-based suspended sediment rating curves, measured using autosampler data and laboratory determinations, for each month from November 2016 to October 2017 and for the full study period.

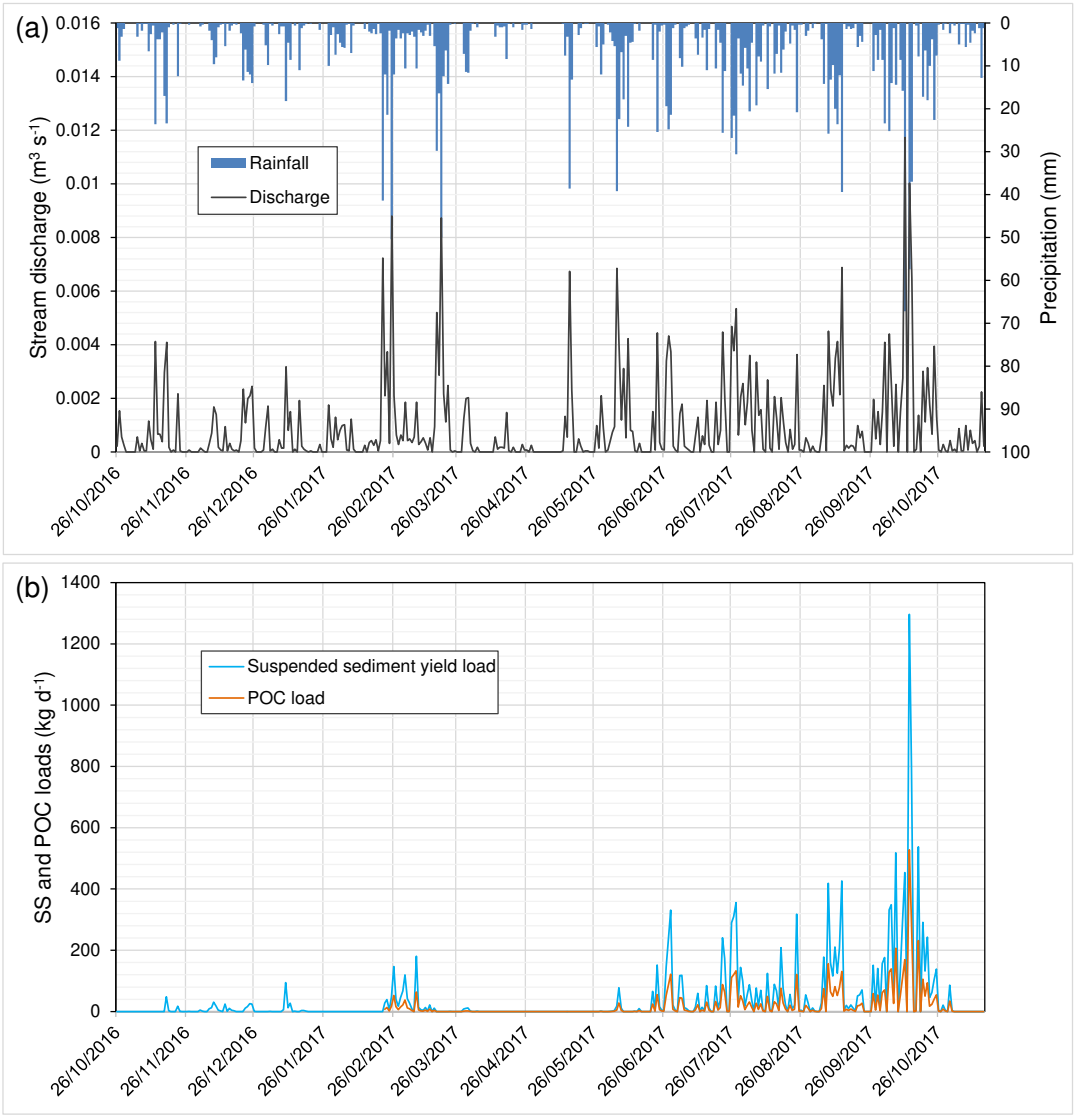

Figure 7. Daily rainfall, discharge, suspended sediment and particulate organic carbon loads during the monitoring period of 26/10/2016–15/11/2017 from the catchment outlet.

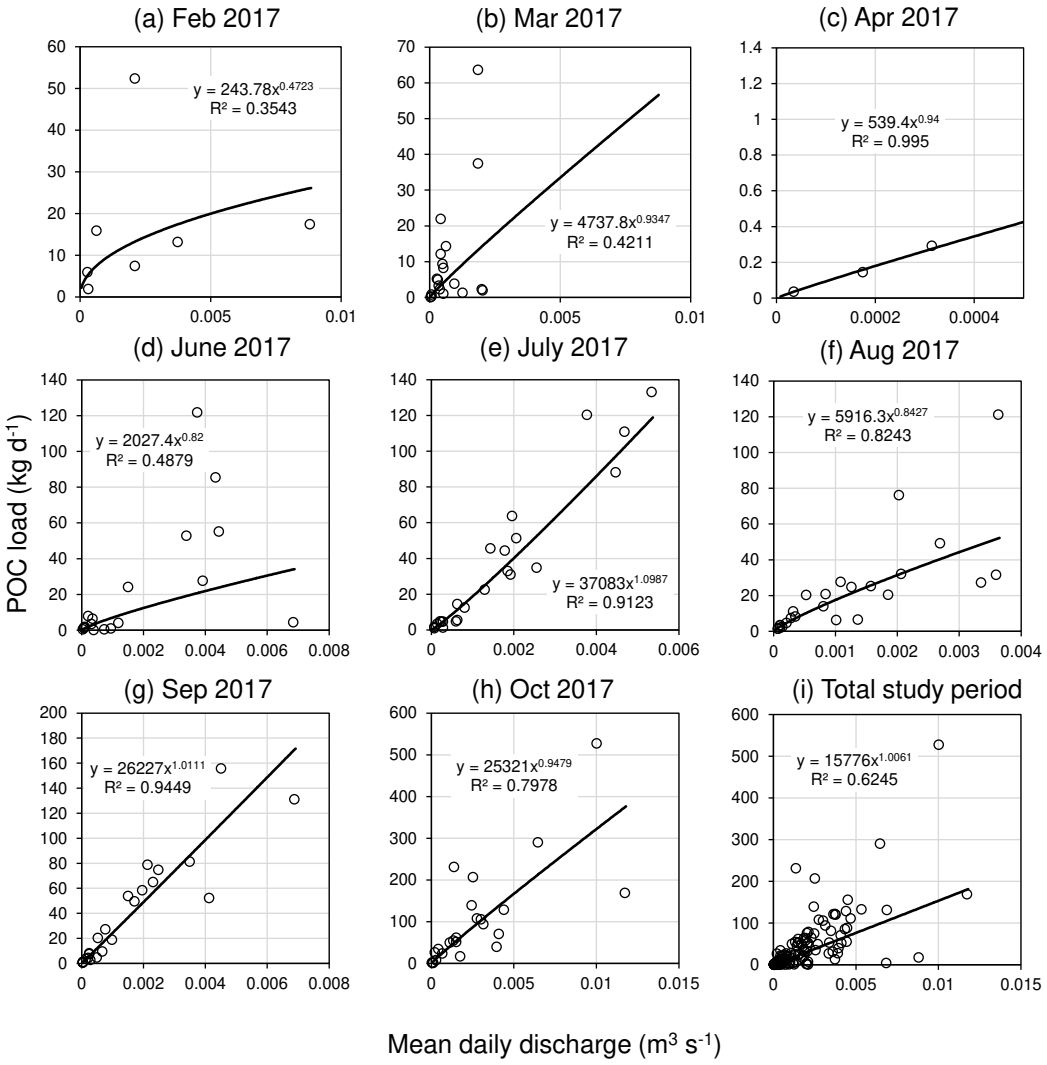

Figure 8. Stream-based POC rating curves, measured using autosampler data and laboratory determinations, for each month from February 2017 to October 2017 and for the total study period.

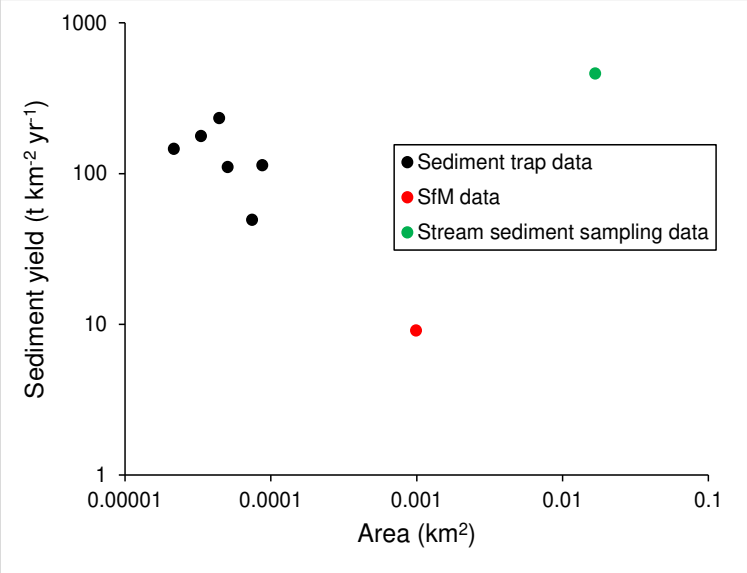

Figure 9. Area-specific sediment yield estimates over the 12-month monitoring period at Fleet Moss, showing the data collection technique used to derive each value.

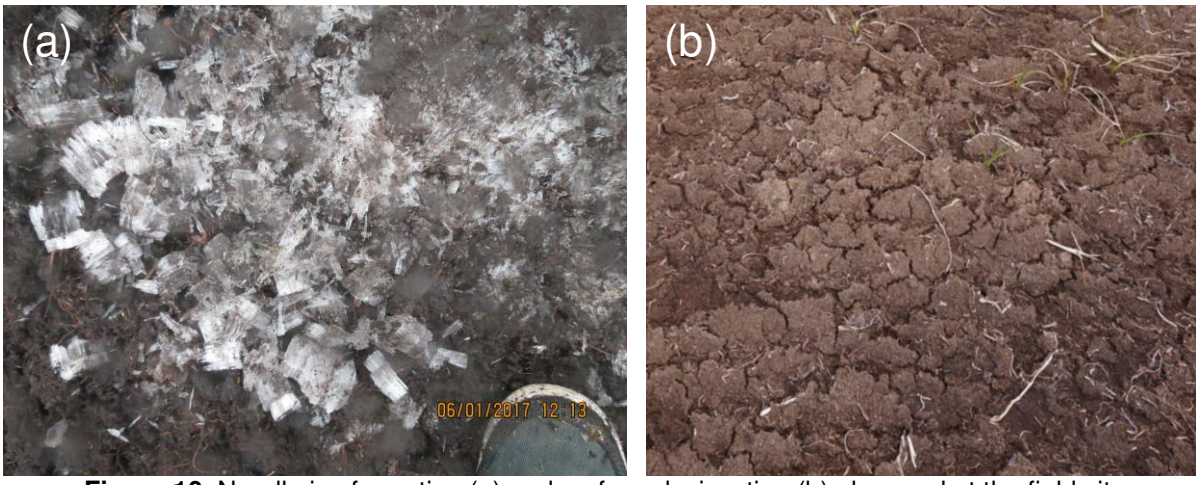

Figure 10. Needle ice formation (a) and surface desiccation (b) observed at the field site.

Graphical abstract

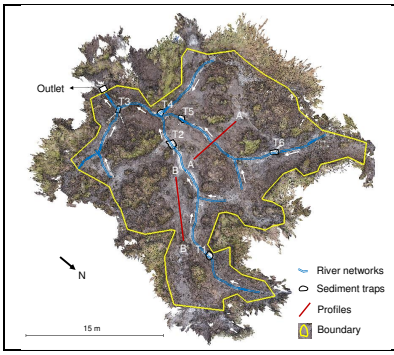

We measured erosion in an upland blanket peatland catchment (0.017 km^2) in northern England using Structure-from-Motion (SfM) photogrammetry, sediment traps and stream sediment sampling. A net median topographic change of –27 mm yr^{-1} was observed over a year by SfM surveys for a small peat catchment. Stream suspended sediment and particulate organic carbon yields were 926.3 t km^{-2} yr^{-1} and 340.9 t km^{-2} yr^{-1} respectively, with highest losses during autumn. The important peat weathering processes were determined.